Journal of the European Ceramic Society 22 (2002) 817–824

www.elsevier.com/locate/jeurceramsoc

Effect of Sb-dopant on phase transitions and selected properties of lead zirconate ceramics

Z. Ujma*, J. Hańderek, M. Kupiszewska

Institute of Physics, University of Silesia, 40-007 Katowice, ul. Uniwersytecka 4, Poland

Received 7 April 2001; accepted 9 June 2001

Abstract

The effect of antimony dopant on AFE–FE and FE–PE phase transitions in the lead zirconate ceramics was investigated by differential thermal analysis, pyroelectric and dielectric measurements. The decrease of these phase transition temperatures was observed without change in width of temperature range in which the intermediate ferroelectric phase occurs. This effect is different from this one observed in the $PbZrO_3$ ceramics with other heterovalent substitutions such as La^{3+}, Ta^{3+} and Nb^{5+} previously studied. The effect of Sb-dopant on $P_r(T)$ and $\varepsilon(T)$ characteristics, and in particular low frequency dielectric dispersion in paraelectric phase is more detailed discussed.

Keywords: Dielectric properties; Ferroelectric properties; $PbZrO_3$; Phase transitions

1. Introduction

Many internal and external factors affect the properties of lead zirconate ($PbZrO_3$), (PZ) single crystals and ceramics, in particular the temperature range below Curie temperature (T_C) in which an intermediate ferroelectric phase (FE) is present. Among the most important internal factors are the uncontrolled or/and intentionally created vacancies in the lead and oxygen sublattices and substitutions for the Pb^{2+} and Zr^{4+} ions. Local electric fields, associated with the heterogeneous distribution of ion defects and mechanical strains play also important role. The applied electric field and pressure are among the most important external factors.

Initially it was thought that pure PZ crystals exhibit only antiferroelectric (AFE) properties below T_C.[1] Some authors also believed that the observed transition to the intermediate FE phase is only due to the presence of certain admixtures.[1,2] The occurrence of this phase is still a matter of debate and an objective of studies.

The most important ferroelectric feature, i.e. the presence of reversible spontaneous polarization (P_s) and the hysteresis loops associated with it was later observed by many authors in a narrow temperature range below T_C.[3–6] Its appearance and disappearance at AFE→FE and FE→PE phase transition temperatures was also proved by pyroelectric measurements.[7,8]

Many investigations tested the hypothesis concerning the influence of vacancies in Pb and O sublattices and of various admixtures on the occurrence of FE phase.[3,9–14] Different substitutions for the Pb^{2+} and Zr^{4+} ions were studied. For a long time the isovalent substitutions were classified into two groups:[15] those which extended the temperature range in which the FE phase occurs (e.g. substitution of Ba^{2+} for Pb^{2+} and Ti^{4+} for Zr^{4+}), those which narrowed this temperature range up to the disappearance of the FE phase (e.g. substitutions of Sr^{2+} and Ca^{2+} for Pb^{2+} and Sn^{4+} for Zr^{4+}).

The heterovalent substitutions can also widen (e.g. Nb^{5+})[11,16] or narrow (e.g. Ta^{5+} and La^{3+})[17,18] this temperature range. Studies of the influence of Sb^{5+} dopant on phase transitions and the selected properties of PZ ceramics are the aim of this paper. Phase transitions were studied by measurements of DTA curves, hysteresis loops, pyroelectric effect, dielectric constant and electric conductivity in the temperature range from the surroundings of the AFE–FE–PE phase transitions. A notable difference of the Sb influence in comparison with the above mentioned heterovalent substitutions

* Corresponding author. Tel.: +48-32-588211x1134; fax: +48-32-588431.

E-mail address: ujma@us.edu.pl (Z. Ujma).

0955-2219/02/$ - see front matter
PII: S0955-2219(01)00399-5

could be expected owing to the differences in their valences, ionic radius and quantum states of valence electrons.

2. Ceramics preparation and their grain structure

The PZ ceramics with Sb contents of 0.2–2 at.% were prepared using the conventional mixed-oxide sintering technique. The PbO, ZrO_2 and Sb_2O_5 oxides containing less than 10^{-2} impurities were used in the synthesis process. The ceramics $PbZrO_3 + xSb_2O_5$, with $x = 0.1$–1 mol% which give 0.2–2 at.% of Sb in the Zr sublattice, were obtained. The synthesis process of the mixed and pressed oxides was carried out at 900 °C. The crumbled, milled and sieved materials, obtained in the synthesis process, were pressed again in the form of cylinders and then sintered at 1100 °C for 2 h. This procedure was repeated before the final sintering at 1260 °C for 12 h. The two sintering processes were performed in a double corundum crucible with interior $PbO + ZrO_2$ atmosphere to prevent sublimation of PbO at high sintering temperatures.

The Sb-doped PZ ceramics, prepared in this way, showed small porosity and good mechanical and dielectric properties. The ceramics with the highest contents of Sb were semitransparent. The Archimedes displacement method with distilled water was employed to evaluate the ceramics density. The observed decrease of density with the increase in Sb-content (Fig. 1) is probably caused by the formation of vacancies in Pb sublattice to obtain electric neutrality of the crystals.

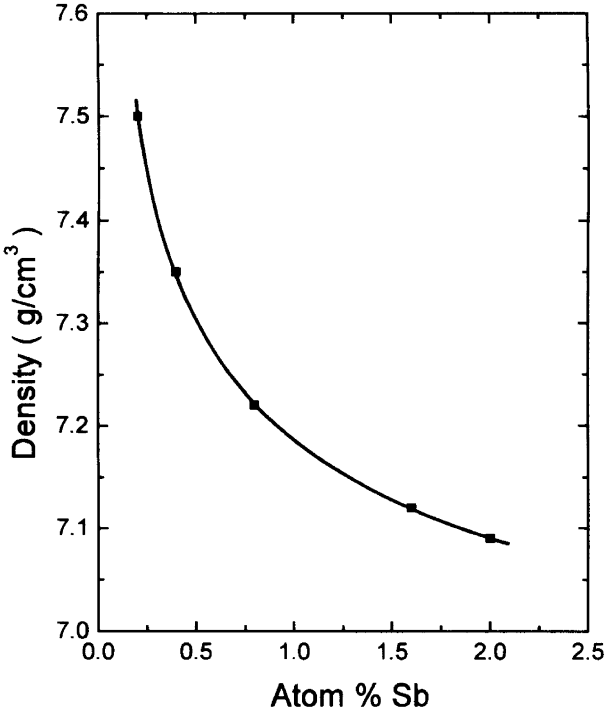

Fig. 1. Density of PZ ceramics vs. Sb content.

The scanning electron microscope JSM-5410 with an energy dispersive X-ray spectrometer (EDS) was used for the investigation of the grain structure and to control the composition of the obtained ceramics. Images of the microstructure on the fracture surface of the ceramics with 0.2 and 2 at.% of Sb-dopant are shown in Fig. 2(a) and (b), respectively. A distribution of the grain size was observed in all the studied ceramics. The increase of Sb concentration causes regular decrease of the average grain size from 10 to 4 μm for the Sb-contents 0.2 and 2 at.%, respectively. The EDS analysis indicates a fairly homogeneous distribution of all the elements (Pb, Zr, O and Sb) throughout the grains.

Samples of appropriate sizes were prepared for the pyroelectric, dielectric and other measurements. The cut and polished samples were coated with silver electrodes, using a silver paste without thermal treatment.

3. Differential thermal analysis

The differential thermal analysis (DTA) was used to determine the temperatures of AFE–FE and FE–PE

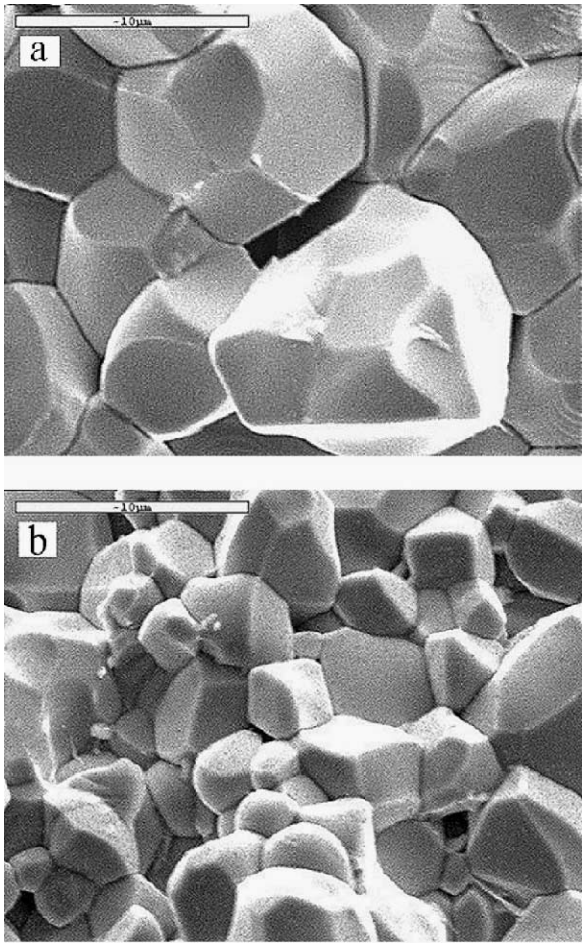

Fig. 2. SEM images of the fracture surface of PZ ceramics with 0.2 at.% (a) and 2 at.% (b) of Sb contents.

phase transitions, in absence of an external electric field, and to detect latent heat of these transformations. Due to the elimination of the electric field the recorded changes of phase transition temperatures caused by the Sb dopant were unaffected by its influence. These investigations were performed with the use of the derywatograph system.

Comparison of DTA curves, obtained on heating and on cooling of PZ ceramics with 0.2 at.% of Sb, is shown in Fig. 3. All the studied ceramics exhibit the presence of two phase transitions both on heating and cooling. However, the DTA curves were ever more broaden with the increase of Sb contents, particularly, in the AFE-FE phase transition. The temperatures corresponding to the maximum in the DTA curves as a function of the Sb-contents are shown in Fig. 4 for the heating run. The AFE–FE and FE–PE phase transition temperatures decrease similarly with increase of Sb contents. So the width of temperature range in which the intermediate FE phase was present does not depend on the Sb contents. In the case of ceramics with a greater Sb-contents, the diffuse character of the AFE–FE and FE–PE phase transitions makes it difficult to separate the maxima of the DTA curves and to determine the latent heat of both phase transformations in this way. It could be estimated for the PZ + 0.2 at.% Sb ceramics using the data shown in Fig. 3. The values of latent heat and changes of entropy of the two studied transformations, determined for cooling are the following $Q_{\mathrm{FE-AFE}} = 508$ J/mol, $Q_{\mathrm{PE-FE}} = 1037$ J/mol and $\Delta S_{\mathrm{FE-AFE}} \cong 1.05$ J/mol K, $\Delta S_{\mathrm{PE\text{-}FE}} \cong 2.1$ J/mol K.

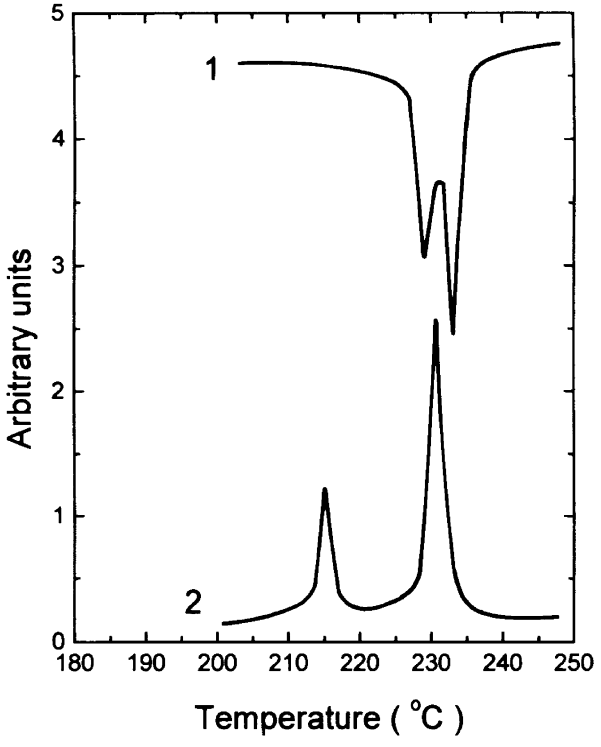

Fig. 3. DTA curves obtained on heating (1) and cooling (2) of PZ ceramics with 0.2 at.% of Sb.

4. Measurements of spontaneous polarization

4.1. Pyroelectric measurements

The ferroelectric nature of the intermediate phase, in between the AFE and PE, was proved by pyroelectric and hysteresis loops measurements. The pyroelectric effect was observed after initial polarization of the studied ceramics in DC field of strength 5kV/cm, applied for $t_p = 20$ min at $T_p = 250$ °C i. e. in PE phase. The samples were then cooled in the field up to the temperature within the range of the FE phase at which the field was switched off. The polarized samples were subsequently heated with a constant temperature rate 5 K/min through the FE–PE phase transition temperature. The pre-polarization procedure was then repeated and after that the samples were cooled through the temperature of the FE–AFE phase transition. The peaks of pyroelectric current, associated with the disappearance of spontaneous polarization during these phase transformations, were recorded with the use of a computerized measuring system. The recorded pyroelectric current vs. temperature and time enabled the determination of the temperature dependence of the pyroelectric coefficient ($\gamma = \mathrm{d}P_s/\mathrm{d}T$) for all the studied ceramics (Fig. 5). In case of samples with Sb contents 1.6 and 2 at.% a particular strong broadening of the FE–AFE

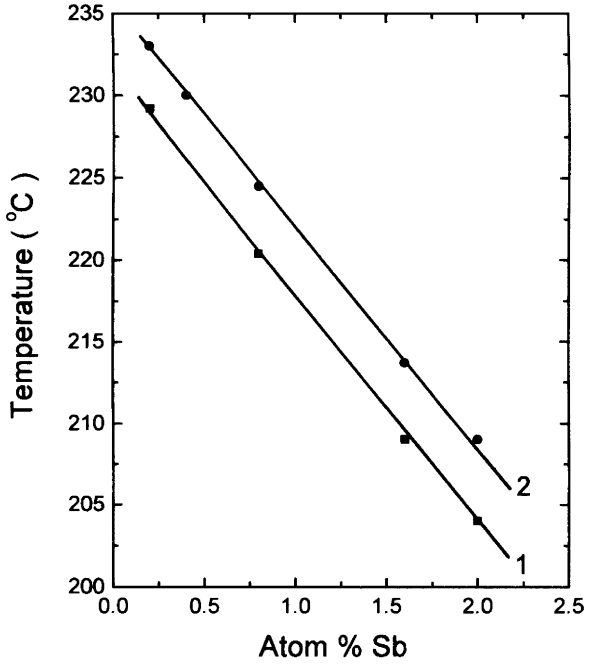

Fig. 4. Temperatures corresponding to the maximum in the DTA curves on heating as a function of Sb-contents. Curves 1 and 2 relate to AFE–FE and FE–PE phase transitions, respectively.

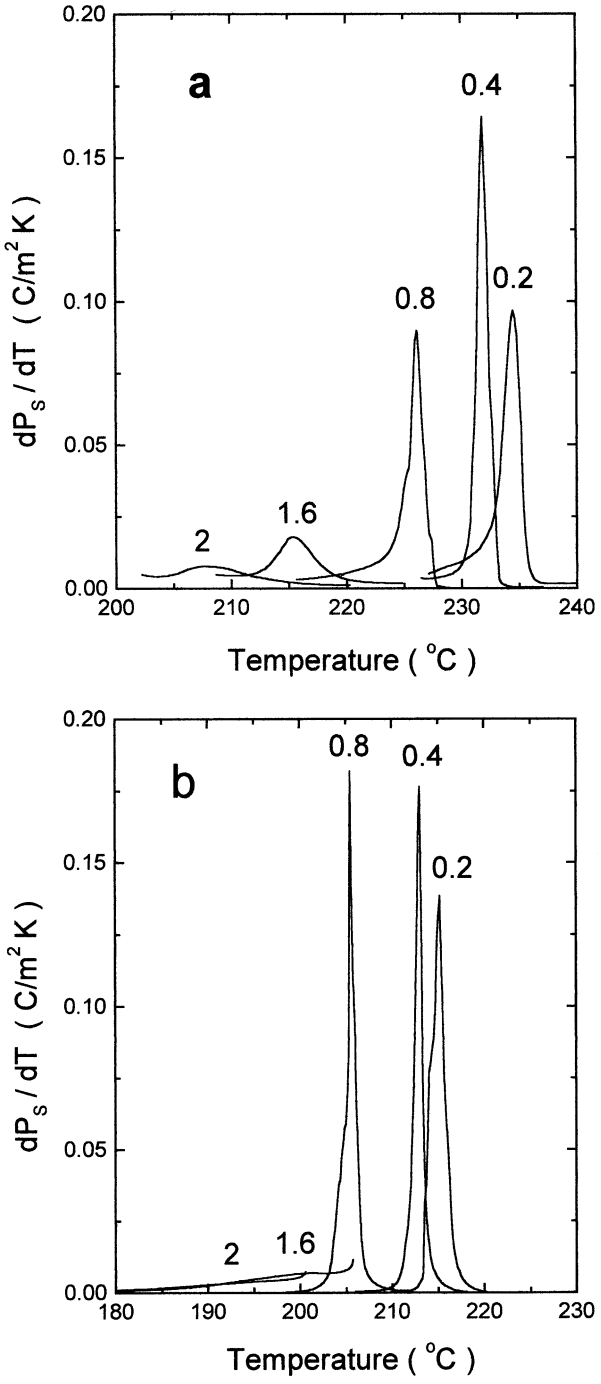

Fig. 5. Temperature dependence of the pyroelectric coefficient determined for the studied ceramics on heating (a) and cooling (b).

phase transition made it impossible to determine the $\gamma(T)$ dependence in the vicinity of this phase transformation on cooling [Fig. 5(b)]. The peaks of the pyroelectric current and coefficient made it possible to determine approximate values of the temperatures of the FE–PE and FE–AFE phase transitions. The temperatures obtained in this way differ slightly from those extracted from the DTA data (Fig. 4). The observed increase and decrease in temperatures of the FE–PE and FE–AFE phase transitions, respectively, probably results from the influence of the indispensable pre-poling procedure of the studied ceramics, applied before the pyroelectric measurements.

4.2. Investigations of the hysteresis loops

The ferroelectric nature of the intermediate phase, which occurs below T_C, was directly determined by investigating the phenomenon of electrical hysteresis. The computerized automatic modified Diamant, Drenck and Pepinsky measuring system was used for the investigation of the hysteresis loops within the temperature range between the mentioned transformations. For a field with a frequency of 50 Hz and an amplitude 8 kV/cm fully saturated electrical hysteresis loops were observed for all the investigated Sb-doped PZ ceramics.

The measuring system made it possible to determine the values of the remanent spontaneous polarization (P_r) on the basis of the observed saturated hysteresis loops. Temperature variation of the spontaneous polarization established in this way, for the heating and cooling processes, are shown in Fig. 6 for the chosen Sb-doped PZ ceramics. The course of the $P_r(T)$ curves differs markedly for the ceramics with a small and higher Sb contents, particularly in the vicinity of the AFE–FE phase transition temperature. The P_r rises relatively fast on heating and cooling in samples with smaller Sb contents [Fig. 6(a) and (b)], whereas it decreases slowly during the strongly diffused FE–AFE phase transition in ceramics with a greater Sb contents [Fig. 6(c)]. Strong broadening of the AFE–FE transformation was also seen in the DTA and $\gamma(T)$ curves. All the investigated ceramics show relatively steep changes of P_r in the vicinity of T_C. The coercive field decreased linearly on heating within the FE phase for all the studied ceramics. The phase transition temperatures, obtained from the $P_r(T)$ curves on heating and cooling, are shown in Fig. 7 as a function of Sb-content.

5. Dielectric measurements

An automatic system was used to measure the dielectric constant (ε) at several frequencies of the measuring field as a function of temperature. These measurements were carried out on heating and cooling with a constant rate of 2 K/min. Comparison of $\varepsilon(T)$ curves, obtained on heating and cooling at the measuring field of frequency 1 kHz for PZ + 0.2 at% Nb ceramics is shown in Fig. 8(a). Steep increase of the $\varepsilon(T)$ curve on heating occurs when approaching the AFE–FE phase transition and a sharp maximum in this curve occurs at the temperature of FE–PE phase transition. Similar behaviour of the $\varepsilon(T)$ curve was observed on cooling but a distinct anomaly in the $\varepsilon(T)$ curves appears in the vicinity of

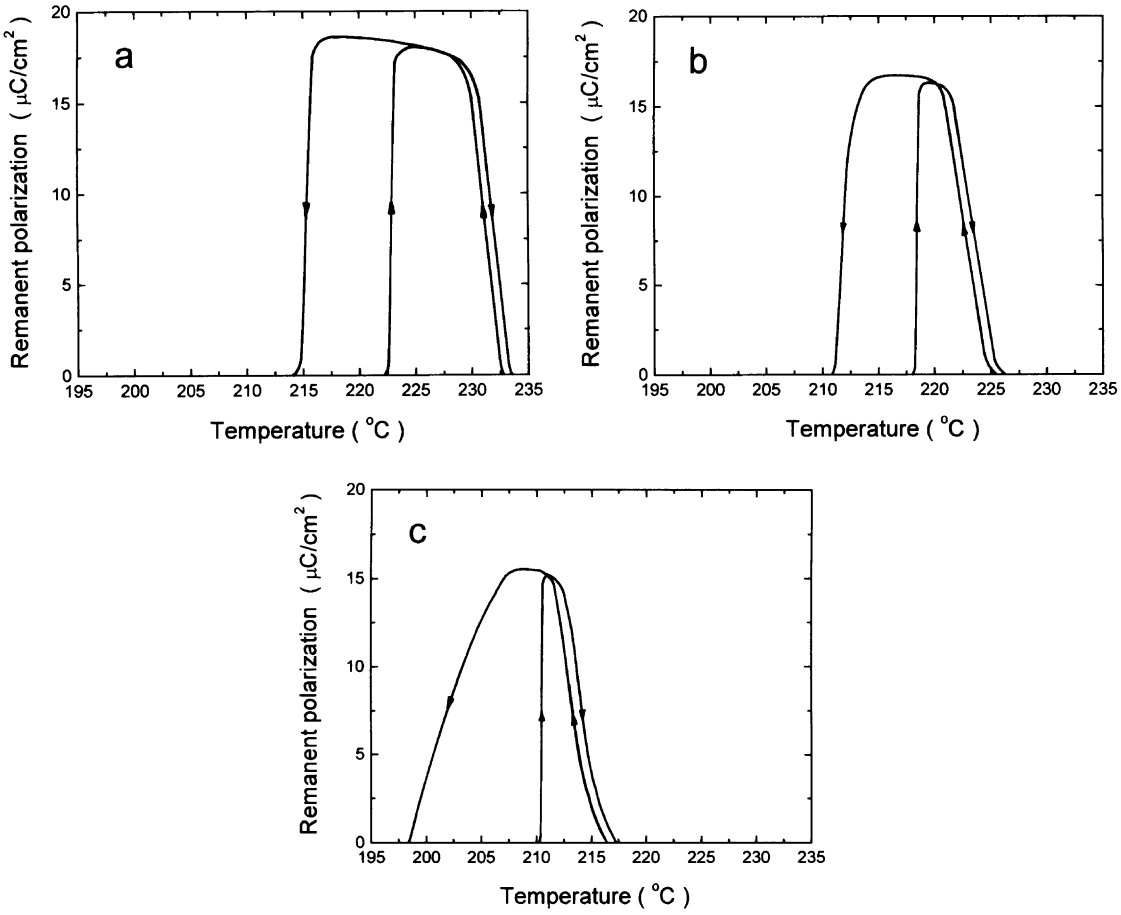

Fig. 6. Remanent polarization vs. temperature, obtained from hysteresis loop measurements on heating and cooling, for PZ ceramics with 0.2 at.% (a), 0.8 at.% (b) and 1.6 at.% (c) of Sb-contents.

FE→AFE phase transition. An accurate estimation of the AFE–FE phase transition temperatures from the $\varepsilon(T)$ curves was impossible for all the investigated ceramics contrary to the FE–PE phase transition temperature.

The characteristics $\varepsilon(T)$ for a number of frequencies of the measuring field are shown in Fig. 8(b)–(d) for the ceramics with Sb contents 0.2, 0.4 and 1.6 at.%. These data are typical for PZ ceramics with the low medium and large Sb contents. The $\varepsilon(T)$ characteristics are weakly frequency dependent within the ranges of AFE and FE phases. In contrast additional maxima in the $\varepsilon(T)$ curves, seen in the PE phase far beyond the Curie temperature, are strongly frequency dependent, at least in some of the studied ceramics. It should be noted that the additional anomalies in $\varepsilon(T)$ curves are, particularly distinct, especially in ceramics with a greater Sb content [Fig. 8(d)]. The plot of the natural logarithm of the measuring frequency vs. reciprocal temperature $T_{\min}$, at which dielectric constant attains local minima, shows an exponential dependence $f=f_0\exp(-E_a/kT_{\min})$ with activation energy $E_a=0.7$ eV. The low frequency dispersion in PE phase practically disappears in samples with the medium Sb contents (0.4 and 0.8 at.%) [Fig. 8(c)]. It

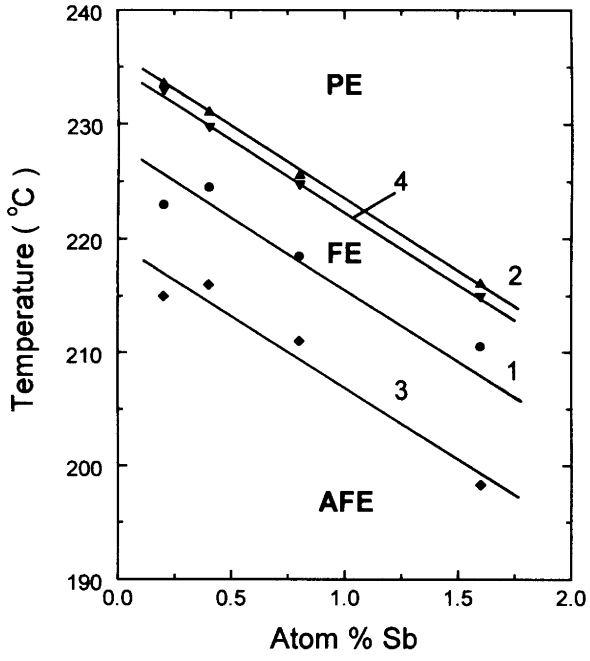

Fig. 7. Variations of AFE–FE and FE–PE phase transition temperatures, determined from $P_r(T)$ measurements, vs. Sb-contents. The curves 1, 2 and 3, 4 relate to heating and cooling, respectively.

does not occur in the studied ceramics at the frequency of 10^4 Hz.

6. Electric conductivity

Additional measurements of electric conductivity vs. temperature in the range from PE phase (300–400 °C) were carried out in order to attain a better understanding of the influence of the Sb dopant characteristics shown above and, in particular, the observed dielectric anomalies far beyond the Curie temperature (Fig. 8). Weak DC field (10 V/cm) was applied to measure the electric conductivity (σ). The results obtained are shown in Fig. 9(a), in the form of dependence $\ln\sigma$ vs. $1/T$, for two of the investigated ceramics. The linear character of this dependence made it possible to determine the activation energy (E_a) of current carriers, responsible for conductivity in the PE phase. The obtained values of the E_a were found to be 1.0 and 1.2 eV for the ceramics with 0.2 and 1.6 at.% Sb contents, respectively. The values of σ at a chosen constant temperature $T=400$ °C vs. Sb content are shown in Fig. 9(b).

In the Sb-doped PZ ceramics the effect of reduction of p-type conductivity could be expected to be similar to the one observed in Nb-doped PZ ceramics.[16] To check this hypothesis the thermoelectric measurements of Seebeck coefficient (α) were carried out at a number temperatures from the mentioned range. The values of α at $T=400$ °C are shown in the Fig. 9(b). Most of the investigated ceramics show p-type conductivity (with a positive sign of α). It is worth noting that p-type conductivity with $\alpha=950$ μV/K was observed in the undoped PZ ceramics.[6]

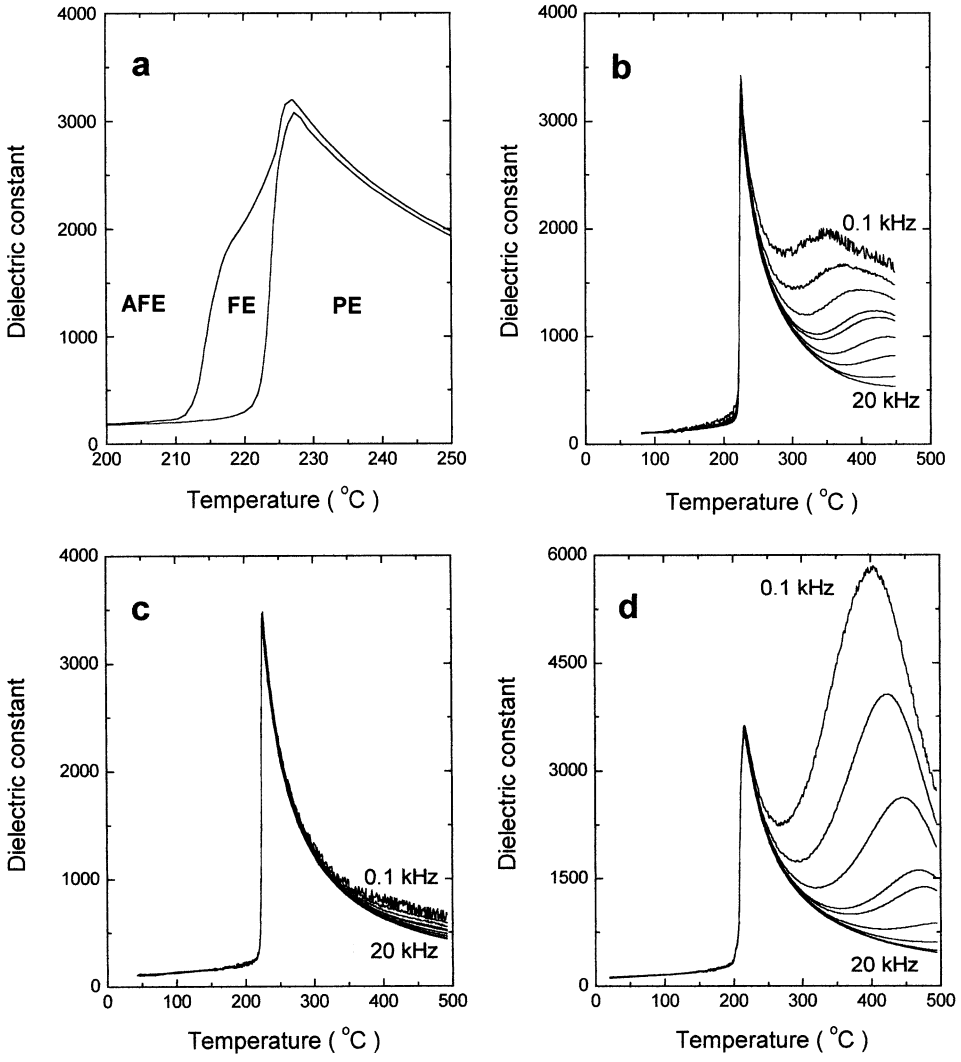

Fig. 8. Dielectric constant as a function of temperature, measured on heating and cooling at frequency of measuring field 1 kHz, for the PZ ceramics with 0.2 at.% of Sb (Fig. 8a). Fig. 8(b)–(d) relate to $\varepsilon(T)$ curves measured at frequencies: 0.1, 0.2, 0.4, 0.8, 1, 2, 4, 10, and 20 kHz on heating for the PZ ceramics with Sb contents (b) 0.2 at.%, (c) 0.4 at.% and (d) 1.6 at.%.

7. Discussion

Various substitutions of five valence elements for Zr^{4+} ions lead to significant changes of phase transition temperatures and even of the phase sequence. Lowering of AFE–FE and FE–PE phase transition temperatures and widening of the temperature range, in which the FE phase occurs, was observed in case of the substitution of a small amount of Nb^{5+} for Zr^{4+} up to about 2 at.%.[16] Narrowing of this range up to the disappearance of the FE phase was, on the contrary, observed in case of the Ta^{5+} substitution for Zr^{4+},[17] despite the fact that both ion radii (R^{5+}_{Nb} = 0.69 Å and R^{5+}_{Ta} = 0.68 Å) and the structural tolerance factor (t_{Nb} = 0.88 and t_{Ta} = 0.884) are very similar. The influence of the Sb^{5+} substitution for Zr^{4+} (R^{5+}_{Sb} = 0.62A, t_{Sb} = 0.91) is also different. Decrease of the AFE–FE and FE–PE phase transition temperatures was observed, as in the case of Nb^{5+} substitution, however, the width of the narrow temperature range in which FE phase occurs remains constant. The difference in atomic weight and, in particular, in the quantum states of valence electrons of Nb, Ta and Sb elements must be responsible for their different influence on phase transition temperatures and even on the phase sequence.

All the above mentioned dopants have at least one common feature. When introduced into the Zr sublattice they create supplementary vacancies in the Pb sublattice to attain electric neutrality of the crystal. The ionised Nb, Ta or Sb atoms together with lead vacancies (Pb) play the role of dipoles, which can behave as nucleation centres of FE domains. Benguigui[10,11] shows that the Nb^{5+}- (Pb) dipoles have a relatively big correlation radius. Hence, they can be responsible for clusters forming of the FE phase in the AFE or PE matrix and consequently for the broadness of the AFE–FE and FE–PE phase transitions. These polar pairs of defects and their bigger complexes are also responsible for the dipole glass behaviour of the material in the PE phase, even far beyond the phase transition temperature region. The accompanying changes in dielectric and pyroelectric properties can be expected both in the vicinities of the AFE–FE and FE–PE phase transitions and within the PE phase. Such changes were in fact observed in PZ ceramics doped by Nb_2O_5,[16] Ta_2O_5[17] and Sb_2O_5 investigated in this paper (Figs. 5, 6 and 8).

The $PbZrO_3$ crystals and ceramics usually contain vacancies in the Pb and O sublattices formed by PbO sublimation in technological conditions of their preparation. Both of them exert a strong influence on the phase transitions and electric properties of these materials, as shown in our earlier papers.[12–14] The PZ ceramics normally exhibits p-type conductivity,[6] for which the Pb vacancies, as acceptors, are mainly responsible. The obtained results show that also PZ ceramics with lower contents of Sb exhibit this type of conductivity. The Sb^{5+} ions substituted for Zr^{4+} ions can be considered as donors. They initially lead to the decrease of conductivity [Fig. 9(b)] due to compensation of the predominant hole current carriers. Further increase of Sb concentration causes increase of conductivity with its simultaneous change towards n-type conductivity due to the increase in concentration of electrons originating from donors [Fig. 9(b)].

Most of the Sb substitutions for the Zr sublattice are not ionised at low temperatures and hence do not give rise to the dipole moments of Sb^{5+}-(Pb) pairs of defects or more complex groups of these defects. The Sb substitutions as donors become more ionised at higher temperatures, and the Sb ions give rise to the resultant dipole moment of the Sb^{5+}-(Pb) pairs of defects. This occurs also in bigger microregions hosting such defects. The materials start to behave as dipole glass in this state, forming additional maxima on the $\varepsilon(T)$ curves in the PE phase region. Such reasoning explains the low frequency dispersion observed in this temperature range. A relatively weaker

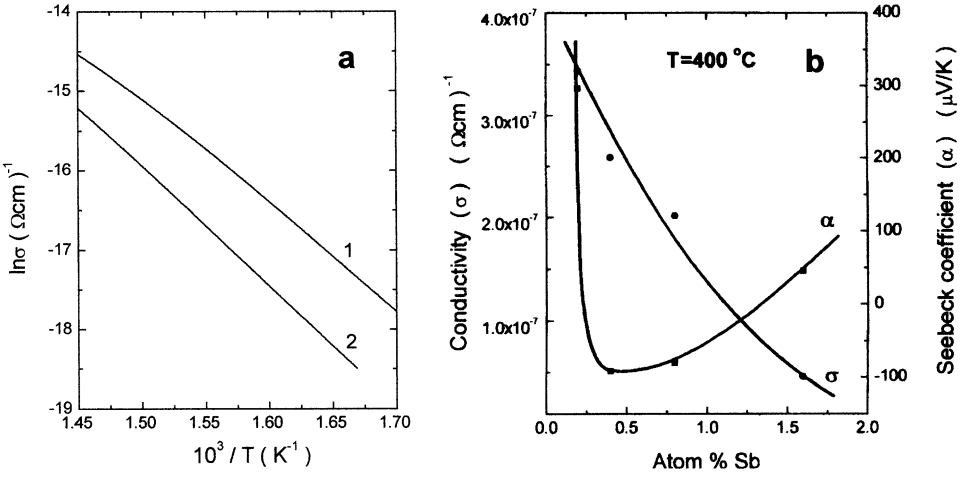

Fig. 9. The natural logarithm of electric conductivity vs. inverse temperature (a) for the PZ ceramics with 0.2 at.% of Sb (curve 1) and 1.6 at.% of Sb (curve 2) and variations of electric conductivity and Seebeck coefficient vs. Sb contents, determined at (b) T = 400 °C.

effect was observed in PZ ceramics with 0.2 at% of Sb while it was much more distinct in ceramics with 1.6 and 2 at.% of Sb. In case of ceramics with 0.4 and 0.8 at.% of Sb the additional anomalies of the $\varepsilon(T)$ curves practically disappear [Fig. 8(c)]. The correlation between these anomalies and the increase of electric conductivity [Fig. 9(b)], accompanied by thermal generation of current carriers from the donors and acceptors is worth nothing here. It associates both vacancies in the Pb and O sublattices with the defects induced by heterovalent substitutions for Zr sublattice, as shown in the present paper and in our earlier papers.[17,19] The process, responsible for the occurrence of the local maxima on the $\varepsilon(T)$ curves in the range of PE phase is of activation character, similarly as in the process of thermal generation of electron-hole current carriers, and gives rise to the increase of electric conductivity. This fact supports the reasoning, which associates the appearance of resultant dipole moments of the pairs and more complex groups of defects.

References

1. Shirane, G., Sawaguchi, E. and Takagi, Y., Dielectric properties of lead zirconate. *Phys. Rev.*, 1951, **84**, 478.
2. Sawaguchi, E., Ferroelectricity versus antiferroelectricity in the solid solutions of $PbZrO_3$ and $PbTiO_3$. *J. Phys. Soc. Jpn.*, 1953, **8**, 615.
3. Golpeau, L., Montagner, S. and Levrel, P., Sur la double transition du zirconate de plomb. *C. R. Acad. Sci.*, 1965, **261**, 2209.
4. Tennery, V. I., High-temperature phase transition in $PbZrO_3$. *J. Am. Ceram. Soc.*, 1966, **49**, 483.
5. Scott, B. A. and Burns, G., Crystal growth and observation of the ferroelectric phase of $PbZrO_3$. *J. Am. Ceram. Soc.*, 1972, **55**, 331.
6. Ujma, Z. and Hañderek, J., Phase transitions and spontaneous polarization in $PbZrO_3$. *Phys. Stat. Sol. (a)*, 1975, **28**, 489.
7. Ujma, Z. and Hañderek, J., The pyroelectric effect in single crystal and ceramics $PbZrO_3$. *Ferroelectrics*, 1981, **33**, 37.
8. Hañderek, J. and Roleder, K., The influence of space charge polarization on phase transition diffusion in $PbZrO_3$ crystals. *Ferroelectrics*, 1987, **76**, 159.
9. Shirane, G., Ferroelectricity and antiferroelectricity in ceramic $PbZrO_3$ containing Ba or Sr. *Phys. Rev.*, 1952, **86**, 219.
10. Benguigui, L., Influence of impurities on the phases of $PbZrO_3$. *C. R. Acad. Sci.*, 1968, **267**, 28.
11. Benguigui, L., Ferroelectricity and antiferroelectricity in pure and Nb_2O_5-doped lead zirconate. *J. Solid State Chem.*, 1971, **3**, 381.
12. Ujma, Z. and Hañderek, J., The influence of defects in Pb and O-sublattices on dielectric properties and phase transitions in $PbZrO_3$. *Phase Transitions*, 1983, **3**, 121.
13. Ujma, Z., Dielectric properties and phase transitions in $PbZrO_3$ with oxygen vacancies. *Phase Transitions*, 1984, **4**, 169.
14. Ujma, Z., Dmytrów, D. and Hañderek, J., The intermediate ferroelektric phase in $PbZrO_3$ with high concentration of defects. *Ferroelectrics*, 1988, **81**, 107.
15. Smolenskii, G. A., Bokov, W. A., Isupov, W. A., Krainik, N. N., Pasynkov, R. J., Shur, M.S., Segnietoelektriki i antisegnietoelektriki. *Nauka, Leningrad*, 1971.
16. Ujma, Z., Dmytrów, D. and Pawełczyk, M., Structure and electrical properties of $PbZrO_3$ doped Nb_2O_5. *Ferroelectrics*, 1991, **120**, 211.
17. Ujma, Z., Dmytrów, D., Kugel, G. and Hassan, H., Dielectric and Raman studies of Ta doped lead zirconate. *Ferroelectrics*, 1993, **146**, 1.
18. Dai, X., Li, J. and Viehland, D., Weak ferroelectricity in antiferroelectric lead zirconate. *Phys. Rev.*, 1995, **B**(51), 2651.
19. Ujma, Z. and Dmytrów, D., Low frequency dispersion in $PbZrO_3$ with oxygen vacancies. *Ferroelectrics*, 1993, **150**, 351.